

# Time-dependent Effects in the Metallic Phase in Si-MOS: Evidence for Non-Diffusive Transport

V. M. Pudalov<sup>a</sup>, G. Brunthaler<sup>b</sup>, A. Prinz<sup>b</sup>, G. Bauer<sup>b</sup>, B. I. Fouks<sup>c</sup>

<sup>a</sup>*P. N. Lebedev Physics Institute, Leninsky prosp. 53, Moscow 119324, Russia*

<sup>b</sup>*Institut für Halbleiterphysik, Johannes Kepler Universität, Linz, A-4040, Austria*

<sup>c</sup>*Institute for Radioengineering and Electronics, Mochovaya str. 18, Moscow 103907, Russia*

(April 17, 2018)

We have found that the conduction in Si-MOS structures has a substantial imaginary component in the metallic phase for the density range  $6 \times n_c > n > n_c$ , where  $n_c$  is the critical density of the metal-insulator transition. For high mobility samples, the corresponding delay (or advance) time,  $\tau \sim (0.1 - 10)$  ms, increases exponentially as density and temperature decrease. In very low mobility samples, at temperature of 0.3K, the time-lag in establishing the equilibrium resistance reaches hundreds of seconds. The delay (advance) times are approximately  $10^2 - 10^8$  times larger than the overall  $RC$ -time of the gated structure. These results give evidence for a non-Boltzmann character of the transport in the low-density metallic phase. We relate the time-dependent effects to tunneling of carries between the 2D bulk and localized states.

The metal-insulator transition observed in different two dimensional carrier systems [1] is currently in the focus of interest. A number of models put forward for its explanation [2–5] span from a non-Fermi-liquid state [2] to interface traps physics [4,5]. In the latter models, the strong exponential drop in the resistivity at low temperature is a transient temperature effect only. On the experimental side, from measurements at high carrier density [6], the exponential drop was proven not to be related to the ground state conduction, at least for high carrier densities  $n \geq (10 - 15) \times n_c$ .

The involvement of interface traps into the transport may be revealed by studying charging effects, time lag, noise character etc. We present here data evidencing that the time-dependent effects are essential in the metallic phase, even for densities 6 times the critical one,  $n_c$ . We studied in detail four samples with different peak mobility, Si-11 ( $\mu^{peak} = 39,000 \text{ cm}^2/\text{Vs}$ ), Si-22 ( $\mu^{peak} = 33,000 \text{ cm}^2/\text{Vs}$ ), Si-4/32 ( $\mu = 8400 \text{ cm}^2/\text{Vs}$ ), and Si-52 ( $\mu = 1300 \text{ cm}^2/\text{Vs}$ ). For the first three samples, an Al gate film was deposited onto the  $\text{SiO}_2$  layer followed by a post-metallization anneal. The density of trapped carriers (estimated from the threshold voltage [7]), was  $(2 - 3) \times 10^{10} \text{ cm}^{-2}$  for the first two samples, and  $21 \times 10^{10} \text{ cm}^{-2}$  for the third one. In the lowest mobility sample, we increased intentionally the amount of disorder by thermal evaporating an Inconel gate without a subsequent anneal. Beyond the substantial decrease in the mobility, the amount of trapped carriers increased up to  $\sim 60 \times 10^{10} \text{ cm}^{-2}$ . All samples were of the same Hall-bar geometry,  $5 \times 0.8 \text{ mm}^2$ , [7] with gate oxide thickness of  $d_{\text{SiO}_2} = 200 \pm 20 \text{ nm}$ , aspect ratio of  $w/l = 0.32$ , and corresponding capacitance between the gate and 2D layer  $C \approx 690 \text{ pF}$ . The potential and current contacts to the 2D channel were lithographically defined and made by thermal diffusion of phosphorus. The overall device  $RC$ -time, including contact resistance was of the order of  $(1 - 10) \mu\text{s}$ , and was expected to contribute a negligibly small imaginary component to the sample ac-conductance.

Four-terminal ac-transport measurements were carried out in the frequency range 0.3 to 30 Hz with a quadrature lock-in amplifier. In order to eliminate the influence of the resistance of potential probes, we used a battery operated electrometric preamplifier with an input current less than 1 pA. The amplifier phase-frequency characteristic was verified not to contribute to the studied effects. In all samples, we found the time-dependent effects to persist in the metallic phase, far above the critical density. In high mobility samples, the characteristic times were in the ms-range and were measured from a phase shift  $\varphi$  between the voltage drop,  $V_x$ , and the source-drain current,  $I_x$ , as well as from the frequency dependence  $\varphi(F)$ . In low mobility samples, the characteristic times were of order of 1-100 s and were measured directly, by applying a small voltage step on the top of the constant gate voltage and measuring the transient voltage  $V_x$  at a constant current  $I_x$ . In the following, we define the “resistivity”,  $\rho$  as the in-phase component,  $Re((V_x/I_x) \times w/l)$ .

**Measurements with high mobility samples.** Figure 1 shows the phase shift between the ac voltage  $V_x$  and the current  $I_x$ , measured in a high mobility sample at a frequency of 3.8 Hz, as a function of carrier density. The phase shift emerges as the density decreases below  $6 \times 10^{11} \text{ cm}^{-2}$ . This is about 6 times larger than the critical density,  $n_c = 0.95 \times 10^{11} \text{ cm}^{-2}$  for the metal-insulator transition in this sample.

The lower inset of Fig. 1a shows that, as density decreases, the phase shift first is negative (which corresponds to the voltage delay), then becomes positive (voltage advancing), and, finally, becomes again negative close to the critical density. The phase shift increases linearly with ac-current frequency  $F$  and may thus be interpreted as a time delay (or advance, correspondingly),  $\tau = \varphi/(2\pi F)$ . The upper inset in Fig. 1a shows delay time ( $= |\tau|$ ) calculated from the slope of the frequency characteristics, at a fixed temperature of 290 mK, and over the range of high densities where  $\phi < 0$ . As temperature decreases, the phase shift displays more and more

pronounced oscillations as a function of density. The phase shift is reproducible during the same cool-down, however, in different cool-downs the oscillatory details varied on the density scale.

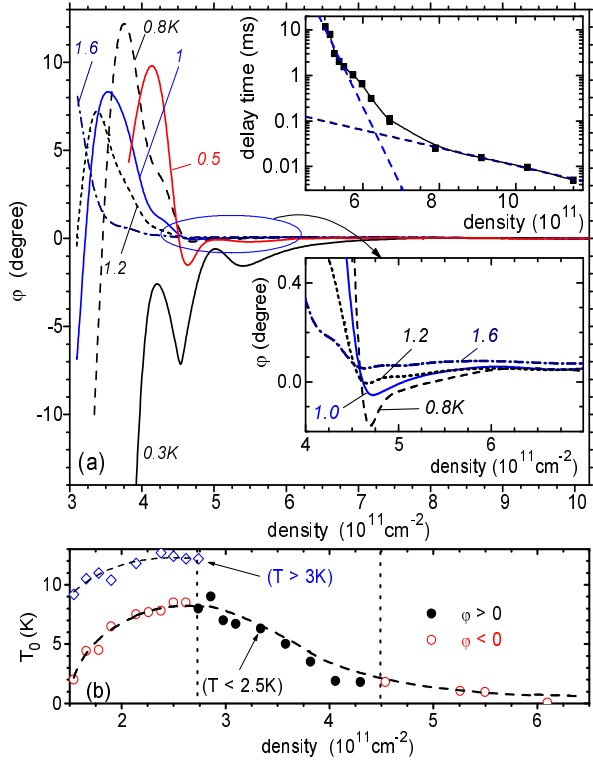


FIG. 1. (a) Phase shift between ac-voltage  $V_x$  and current  $I_x$  measured with sample Si-22 at frequency 3.8 Hz for 6 temperatures (indicated on the figure). The range of  $n = (4 - 7) \times 10^{11} \text{ cm}^{-2}$  is blown up on the lower inset. Upper inset displays delay time vs density, measured from the frequency dependence of the phase shift at  $T = 0.29 \text{ K}$ . (b) “Activation energy”,  $T_0$ , for low and high temperature ranges. Vertical dashed lines  $n = n_i$  separate the regions of positive and negative  $\varphi$ .

Figures 2 a and 2b show the phase shift and the resistivity for sample Si-22 as a function of temperature for eight fixed densities. It is remarkable that *the strong exponential drop in resistivity develops in the same ranges of densities and temperatures as the phase shift does*, although we can not simply relate the two effects to each other.

As follows from Figs. 1a and 2a, both,  $\tau$  and  $\varphi$  decay about exponentially with density and temperature,

$$\tau \propto f_1(n, T) \exp(T_0(n)/T). \quad (1)$$

The prefactor  $f_1$  oscillates as a function of density (and of temperature) changing sign at “node” values,  $n_i$ . The definition of the slope,  $T_0$ , is illustrated by the dashed tangent lines in the lower inset of Fig. 2a.

$T_0(n)$  is not constant over entire temperature range: it is large for high temperatures, and decreases for lower

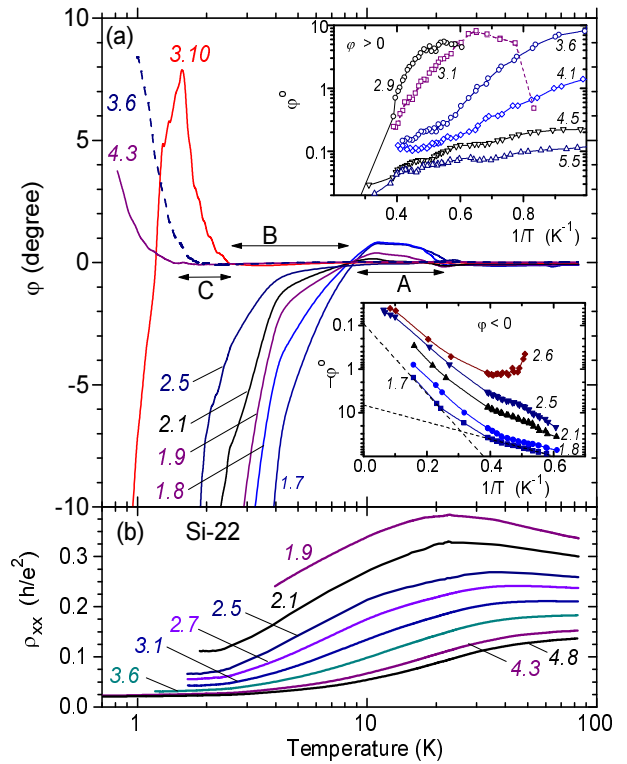


FIG. 2. (a) Temperature dependence of the phase shift,  $\varphi$ , measured at 3.8 Hz for eight different densities (indicated on the figure in units of  $10^{11} \text{ cm}^{-2}$ ). Lower and upper insets are the “Arrhenius plots” for  $\varphi$  vs  $1/T$ : lower inset is for the negative  $\varphi$  over the temperature range “B”; upper inset is for the positive  $\varphi$  over the range “C”. (b) Temperature dependence of the resistivity for the same eight densities as in (a).

$T$ ’s. In the vicinity of the nodes  $n_i$  and for low temperatures, the slope tends to vanish which is simply affected by the oscillatory behavior of  $f_1(T)$ . Therefore, the narrow density ranges around the nodes were ignored in the calculations of  $T_0$ . The resulting density dependence  $T_0(n)$  is shown in Fig. 1b, evaluated separately for high ( $T > 2.5 \text{ K}$ ) and low ( $T < 2.5 \text{ K}$ ) temperatures. Despite Eq. (1) describes the data very roughly, an important conclusion can be drawn immediately:  $T_0$  does not decrease to 0 for the nodes  $n = n_i$  and develops smoothly from the ranges of  $\varphi > 0$  to those of  $\varphi < 0$ . This means that the nodes are related to the prefactor  $f_1(n)$  rather than to the exponential factor. For high densities,  $T_0$  decays steeper than  $\propto (n - n_0)^{-1}$ , as shown in Fig. 1b, thus causing an exponential decay of  $\tau$  for high densities.

**Low mobility sample.** In the low mobility sample Si-52, the time-dependent effects are much stronger and manifest themselves in a transient voltage between potential probes when the gate voltage  $V_g$  changes by a small step  $\Delta V_g \ll V_g$ . Typical transient curves 1 - 5 of  $\Delta\rho(t) = \rho(t) - \rho(0)$  normalized by  $\Delta\rho_0 = \rho(\infty) - \rho(0)$  are shown in Fig. 3a, for 5 different densities. The curves were fitted with exponential functions  $\rho_0 \exp(-t/\tau_d)$  (shown by

dashed curves), from which the time lag  $\tau_d$  was obtained. At some, rather arbitrary densities, the transient curves were non-monotonic with oscillations (curve 6), or jumps (curves 7, 8, 9).

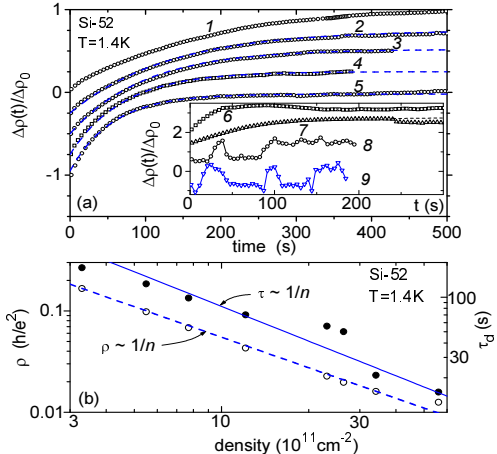


FIG. 3. (a)  $\Delta\rho(t)$ , normalized by  $\rho(\infty) - \rho(0)$ . Curves 1-5 are shifted vertically for clarity. The curves 1-5 correspond to the carrier densities 3.3, 5.5, 7.7, 12.1, 23.1 (in units of  $10^{11} \text{ cm}^{-2}$ ). Curves 6-9 ( $n = 34, 26, 23$ ) in the inset show examples of non-monotonic behavior. (b) Time lag  $\tau_d$  (right  $y$ -axis) and  $\rho$  (left  $y$ -axis) vs carrier density.

The time lag  $\tau_d$  and resistivity  $\rho$  are plotted in Fig. 3b vs carrier density. Their ratio,  $\tau_d/\rho$ , is again  $10^8$  times larger than the sample capacitance pointing to its irrelevance.

**Discussion.** The characteristic times, even for high mobility samples, are of the order of  $10^{-4} - 10^{-2}$  s and, therefore, can not be associated with any  $RC$  time constants of the sample. Having the typical sample parameters  $R \sim (10^3 - 10^4)$  Ohm, and  $C = 0.7 \times 10^{-9}$  F, one can hardly find in the sample either a capacitance  $\sim 10^{-4}$  F, or a resistance  $\sim 10^8$  Ohm (in the metallic range of densities). Only for high densities  $n \gtrsim 20 \times 10^{11} \text{ cm}^{-2}$ , the delay time becomes comparable to  $RC = 10^{-6}$  s. The huge time  $\tau$  can not be attributed to contact phenomena, because for the more disordered sample Si-52, at much higher densities (and for lower resistance of the contacts, correspondingly),  $\tau$  is larger by a factor of  $10^5$ . The irrelevance of the contacts to the time-dependent effects is also confirmed by the linearity of the  $I-V$ -curves measured between different contacts with currents in the range from  $10^{-7}$  down to  $10^{-12}$  A.

**Model.** Interface defect charges originating from the lack of stoichiometry are intrinsic to Si/SiO<sub>2</sub> system; their typical density is  $10^{12} \text{ cm}^{-2}$  for a state-of-art thermally grown dioxide [8]. Tunneling of electrons from Si to the interface charged states is known to cause a time lag in Si-MOS capacitors at room temperature [8]. These charged states are partly neutralized during slow cooling of Si-MOSFETs with a positive gate voltage applied.

Further, at liquid helium temperatures, electron tunneling rate to these interface traps in SiO<sub>2</sub> under a barrier of 3.2 eV is negligible. The uniform part of the potential produced by interface-state charge is out of importance, however, spatial fluctuations of the built-in charge produce shallow fluctuations of the potential acting on 2D electrons in Si (at  $z > 0$ ), and cause corresponding localization of electrons. We assume that the observed times are due to tunneling processes, on the Si-side entirely, between the electrons in 2D “bulk” and the potential traps in the localized areas produced by the fluctuations of the interface charge [9]. For the discussed low-temperature case, the active traps are created by the attractive (positive) charges that fall inside a large-scale repulsive fluctuation. The attractive charge placed at the interface (at  $z < 0$ ) localizes an electron nearby (on the Si-side,  $z > 0$ ), with a binding energy [9]

$$\varepsilon_b = -m^* e^4 / 8\kappa^2 \hbar^2. \quad (2)$$

Here  $m^* = 0.21m_e$  is the electron effective mass,  $\kappa = 7.7$  the average dielectric permittivity, and thus  $\varepsilon_b = 0.02$  eV for the Si/SiO<sub>2</sub> interface. The repulsive charges which are very closely located to the attractive charge, decrease the binding electron energy. As a result, the binding energy distribution broadens and extends over a wide energy range, from about  $\varepsilon_b$  down to 0. The effective binding energy  $\varepsilon_b^{eff}$  is therefore substantially lower than  $\varepsilon_b$ .

The localized state is located inside a large-scale repulsive fluctuation and is surrounded by a broad potential barrier of the height  $\varepsilon_b^{eff}$ . The barrier itself is surrounded by the electrons in the metallic regions of the 2D bulk. The barrier is responsible for the large electron capture and emission times. At nonzero  $T$ , only the traps located close to the Fermi level, within  $E_F \pm kT$ , are recharging when the local potential in the 2D bulk varies.

For low temperatures, the electron emission time [9] equals to

$$\tau_{em} \approx (\hbar/\varepsilon_b) \exp(-x/\lambda), \quad (3)$$

where  $\lambda = \sqrt{\hbar^2/8m^*\varepsilon_b^{eff}}$  is the typical tunneling length and  $x$  is the distance from the trap to the nearest conductive region. The capture time  $\tau_c$  is related to  $\tau_{em}$  by the obvious relationship:  $\tau_c/\tau_{em} = (1-f)/f$ , where  $f$  is the level occupancy (Fermi distribution function). For the traps whose energy is close to  $E_F$ ,  $f \approx 1/2$  and these two times are about equal. Using, for an estimate,  $\varepsilon_b^{eff} = 0.01$  eV we obtain  $\lambda = 20 \text{ \AA}$  and the tunneling distance  $x = 460 \text{ \AA}$  corresponding to the tunneling time  $10^{-3}$  s. Thus, a radius of the repulsive barrier  $r$  is to be of the order of  $500 \text{ \AA}$ , to account for the recharging time of 1 ms. For more disordered samples, the amount of the charge trapped at the interface and the amplitude of potential fluctuations are even larger. Therefore, the radius (in the  $x - y$  plane) of the potential fluctuations is also larger. To account for  $\tau = 100$  s, we estimate  $x$  has to be equal to  $700 \text{ \AA}$ . The length scale,  $(500 - 700) \text{ \AA}$ ,

of the potential fluctuation is consistent with numerous data obtained for similar samples, as well as with direct tunneling microscopy of the Si/SiO<sub>2</sub> interface [10].

As electron density and  $E_F$  increase, the potential barriers get thinner [9] due to screening by free electrons of the 2D bulk, and the radius of the total repulsive fluctuation decreases, causing  $\tau$  to decrease monotonically. This is in a competition with a density dependence of the effective binding energy  $\varepsilon_b^{eff}$ ; as a result, the overall density dependence of  $\tau$  may be non-monotonic. Finally, above a certain density, all localized states sink below the Fermi energy, the barriers are screened entirely, and the Drude-Boltzmann regime sets in replacing tunneling. The onset occurs at Fermi energy equal roughly to the amplitude of bare fluctuations, and is thus inversely proportional to the sample peak mobility.

The temperature comes into the model via (i) the tunneling distance to the nearest trap level found within the energy interval  $E_F \pm kT$ , (ii) Fermi distribution function  $f$  and (iii) activation processes on the border and inside the localized area. These mechanisms lead to temperature dependences  $\tau \propto \exp(-T_{0,i}/T)$ , and the resulting temperature dependence may have different  $T_{0,i}$  in different ranges of temperature.

The electron tunneling time is much larger than the transport scattering time ( $\approx 3$  ps), the electron-electron interaction time,  $h/E_{ee} \sim 0.1$  ps, and the electron diffusion time ( $\approx 20$  ps). Therefore, all electrons in 2D layer do participate in tunneling during a time  $\tau \gtrsim 10^{-3}$  s. The capacitance [11] and Hall voltage [7] are measured at frequencies lower than the tunneling rate,  $1/\tau_{em}$ , hence, all the electrons of the 2D bulk participate in re-charging or in Hall transport.

In summary, our data show that the charge transport in the “metallic conduction” regime is accompanied by (or includes) a non-diffusive component. It manifests itself in the time-dependent effects in metallic phase over density range from  $n_c$  to about 6 times  $n_c$ . The delay/advance time between the ac voltage and the current in high mobility samples is of the ms-range and grows exponentially as density and temperature decrease. For more disordered samples the time lag between the gate voltage pulse and the response reaches 1-100 seconds. We associate these times with the “in-plane” tunneling of carriers between the 2D bulk and the potential traps. The suggested model presumes that the unit “slow” trap consists of a potential well surrounded by potential barrier, and seems to be applicable to various material systems since similar long-range localized areas were found in GaAs/AlGaAs as well [12]. Particularly, this may be relevant to the system with a set of artificial quantum dots (traps) [13]. The model may qualitatively describe (i) large delay time  $\tau$ , (ii) the growth of  $\tau$  as temperature and density decrease, and (iii) the non-monotonic density and temperature dependence of  $\tau$ . Whereas the tunneling time in the above model is different from that in Ref. [4], the physics of the temperature dependence

of the resistivity caused by “fast traps” (located nearby the border between the localized and free carriers) may be similar. The complexity of the presented data, however, requires a thorough theoretical consideration, which should take into account interaction of the free carriers in 2D bulk with the localized ones, recharging and screening processes within the localized areas, and symmetry properties of the surface localized states.

V.P. acknowledges help by M. D'Iorio and E. M. Golliamina in samples processing, and stimulating discussions with B. Altshuler, D. Maslov, and A. Finkelstein. The work was supported by RFBR, by the Programs “Physics of solid-state nanostructures” and “Statistical physics”, by INTAS, NWO, and by FWF P13439 and GME, Austria.

---

[1] S. V. Kravchenko, et al. Phys. Rev. B **51**, 7038 (1995). Phys. Rev. B **50**, 8039 (1994). D. Popović, A. B. Fowler, S. Washburn, Phys. Rev. Lett., **79**, 1543 (1997). Physica B, **249-251**, 701 (1998). P. T. Coleridge, et al. Phys. Rev. B **56**, R12764 (1997). M. D'Iorio, D. Brown, H. Lafontain, Phys. Rev. B **56**, 12741 (1997). Y. Hanein, et al. Phys. Rev. Lett. **80**, 1288 (1998). Phys. Rev. B **58**, R13338 (1998). M. Y. Simmons, et al. Phys. Rev. Lett. **80**, 1292 (1998).

[2] A. M. Finkel'stein, Sov. Sci. Reviews/section A- Physics Reviews, Ed. I. M. Khalatnikov, **14**, 3 (1990). Q. Si, C. M. Varma. Phys. Rev. Lett. **81**, 4951 (1998); D. L. Shepelyansky, Phys. Rev. Lett. **73**, 2607 (1994); cond-mat/9902246. D. Weinmann, J.-L. Pichard, Y. Imry, J. Phys. I **7**, 1559 (1997). D. Belitz, T. R. Kirkpatrick, Phys. Rev. B **58**, 8214 (1998). F. von Oppen, T. Wetting, Europhys. Lett. **32**, 741 (1995). P. Jacquod and D. L. Shepelyansky, Phys. Rev. Lett. **78**, 4986 (1997). T. Vojta, F. Epperlein, M. Schreiber, Phys. Rev. Lett. **81**, 4212 (1998).

[3] V. M. Pudalov, JETP Lett. **66**, 175 (1997).

[4] B. Altshuler, D. Maslov, Phys. Rev. Lett. **82**, 145 (1999).

[5] S. Das Sarma, E. H. Hwang, Phys. Rev. Lett. **83**, 164 (1999). S. Das Sarma, T. Klapwijk, cond-mat/9810349; Sol. St. Comm. (1999).

[6] V. Pudalov, G. Brunthaler, A. Prinz, G. Bauer, Phys. Rev. B **60**, R2154 (1999).

[7] V. Pudalov, G. Brunthaler, A. Prinz, and G. Bauer, JETP Lett. **70** (1999). [Pis'ma ZhETF **70**, 48 (1999)].

[8] T. Hori, *Gate dielectrics and MOS ULSIs*, Springer-Verlag, Berlin, NY, (1997).

[9] B. I. Fuks, Sov. Phys: JETP, **75**, 294 (1992). [ZhETF, **102**, 555 (1992)].

[10] M. S. Khaikin, et al, JETP Lett. **44**, 245 (1986).

[11] S. V. Kravchenko et al., Phys. Rev. B **47**, 12961 (1993).

[12] G. Eytan et al. Phys. Rev. Lett. **81**, 1666 (1998).

[13] R. Ribeiro, et.al. Phys. Rev. Lett. **82**, 996 (1999).